Earth`s Cryopshere, 2018, vol. XXII, No. 3, pp. 16–23 **http://earthcryosphere.ru/**

DOI: 10.21782/EC2541-9994-2018-3(16-23)

RESULTS OF GROUND-PENETRATING RADAR INVESTIGATIONS ON THE NELLA FJORD SEA ICE (PROGRESS STATION AREA, EAST ANTARCTICA) IN THE 2016/17 AUSTRAL SUMMER FIELD SEASON

S.V. Popov[1], V.L. Kuznetsov[2], S.S. Pryakhin[2], M.P. Kashkevich[3]

[1]*Polar Marine Geosurvey Expedition (PMGE), 24, Pobeda str., Lomonosov, St. Petersburg, 198412, Russia; spopov67@yandex.ru*
[2]*Arctic and Antarctic Research Institute, 38, Bering str., St. Petersburg, 199397, Russia*
[3]*Saint-Petersburg University, 7-9, Universitetskaya emb., St. Petersburg, 199034, Russia*

The paper presents the main results of the field investigations using multi-frequency (150 MHz, 270 MHz, 400 MHz and 900 MHz) ground-penetrating radar profiling and georadar sensing by the common depth point method.The investigations have been carried out on the fast sea ice of Nella Fjord (Eastern Antarctica) during the 2016/17 austral summer field season. The studies have included seawater salinity measurements. The sounding of sea ice with thickness of about 1 m thick have proved to be most effective at the radar frequencies which correspond to the wavelengths in a meter range. Besides the intensive reflections from the lower edge of sea ice, the ground-penetrating radar data have revealed a boundary between fresh- and saltwaters whose position has been corroborated by the salinity measurements. The ground-penetrating radar technique in CDP mode has served as a basis for the subsurface velocity model showing that the effective dielectric constant for sea ice equals 10, which is accounted for intense melting of sea ice and its saturation with fresh water. The value of effective permittivity the fresh water layer is found to be 75, which may have been prompted by roughness of the lower edge surface of sea ice.

East Antarctica, Progress Station, ground-penetrating radar sounding, sea ice, common depth point, seawater salinity

INTRODUCTION

The research focused on Arctic and Antarctic sea ice contains both fundamental scientific interest and specifically applied tasks, such as unloading of ships, construction of ice runway for receiving the aircraft and providing for other types of logistics. While considering drilling ice cores to be the most reliable method of studying the natural environments and their evolution, we should admit its complexity: in the context of Antarctica, it is a significant logistical exercise, and requires much effort, time and patience from the researchers. Besides, this method allows acquiring information only from selected points, whereas geophysical surveys provide more complete information along the profile even after drilling. In this sense, electromagnetic soundings recognized as highly efficient and economic operations, appear more attractive.

The numerous publications devoted to the GPR studies of sea ice not only provide results of field measurements, but also discuss the theoretical aspects of this method. Among them, the most recent and significant publications are: [*Finkelshtein et al., 1977; Haas et al., 1997, 2009; Lebedev and Sukhorukov, 2001; Haas, 2004; Bobrov et al., 2008; Galley et al., 2009; Holt et al., 2009; Panzer et al., 2010, 2013; Lee et al., 2011*]. Despite all its advantages of this progressive geophysical method, however, the GPR technique has a number of drawbacks. In particular, due to high conductivity of seawater, it creates a shield for electromagnetic waves, impeding thereby the radar's penetration to the entire ice thickness. This circumstance largely constrains the range of the GPR applicability within the focus of this discussion. Besides, the applied interest in sea ice is related primarily to the summer field season, which is coincident with the peak of logistical activities in Antarctica. However, on account of the specific environmental conditions of polar latitudes, this time period is also associated with the onset of the intense melting of sea ice, promoting its significant saturation with fresh water and, as a result, the desalination of the surface layer of sea water. The effect of fresh water consists in reducing salinity and therefore conductivity of sea ice, and ultimately, the shielding properties of seawater, making it possible to effectively use electromagnetic methods.

The experimental verification of the above considerations was implemented through the acquisition tests (AT) performed on the sea ice of Nella Fjord near Russian research station Progress (East Antarctica) during the austral summer field season of the 62nd Russian Antarctic Expedition (RAE, 2016/17), which encapsulated the research works commenced during the 60th RAE season (2014/15) in the area of the Molodyozhnaya field base [*Popov and Polyakov, 2015*] and continued in the RAE 61st season (2015/16).

MULTI-FREQUENCY GPR PROFILING

The works were carried out on January 5, 2017 on the AARI multi-year oceanographic profile in the point with coordinates 69°22.869′ S, 76°21.777′ E (Fig. 1, *a*). Prior to commencement of the AT works, a traverse line marked point-to-point throughout its length (20 m), with its center located in the vicinity of the ice-hole (maina), the remnant of the arrangements for oceanographic measurements taken a day earlier (Fig. 1, *b*). The GPR profiling was performed at several frequencies: 150, 270, 400 and 900 MHz. The first and third frequencies were intended for the "OKO-2" GPR (LLC "Logic systems", Russia) using antennas AB-150 and AB-400M, respectively [*Radiotechnical device..., 2009*]. The extensible antenna AB-150 can be used for multi-offset GPR sounding. Investigations at the frequencies of 270 and 900 MHz was performed using GSSI GPR (Geophysical Survey Systems Inc., USA) with SIR-3000 system module and accordingly 50270S and 3101 antennas [*GSSI..., 2014*]. The tools were carried while walking at a steady pace along the profile.

Figure 2, *a* shows a 150 MHz frequency GPR time-section. Due to the presence of correlated noise of unknown origin, the filtering was performed using horizontal window of 100 traces. The observed reflections are characterized by a mosaic structure with poorly distinguished two partially filter-suppressed boundaries *1* and *2* located in the immediate proximity to the maina, at 26.6 and 42.3 ns delays, respectively (Fig. 2, *a*).

The bottom part shows a large number of diffraction events *3*, which may have been caused by diffraction from the ice blocks at the lower edge of the sea ice. A.L. Novikov, the oceanologist from Mirny station (*private communication*), believes that they can be linked with the anchor ice for whatever reason floated up beneath the surface ice. The diffraction points are not distinctly discernible in the section, however, if the branches of the hyperboles generated for diffracted waves were extended upwards, these will be found in the interval between boundaries *1* and *2*, which allows an inference that the first one is related to the "ice–water" interface.

Diffracted wave *4* identified on the time section (Fig. 2, *a*) with its position corresponding to the profile center, but slightly lower with respect to boundary *2*, was probably reflected by the lower part of the ice-hole. The shift of apex *4* below the assumed ice-water boundary may be due to the GPR track slightly deviating from the hole, without passing directly above it (Fig. 2, *b*), which results in an increase of a raypath to the reflector [*Popov and Kashkevich, 2015*]. Besides, the reflection is likely associated not with the hole itself, but with fragments of ice generated during its cutting and localized in the low-velocity water column. There is no other evidence for the ice-hole on the time section.

Figure 2, *b* represents by a 270 MHz frequency GPR time section resulted from horizontal filtering of 100 tracks, exhibiting numerous subhorizontal reflection events (probably including re-reflections) produced by the sea ice and, assumingly, by the medium (seawater). The previously identified boundaries *1* and *2* are present among them. Note that they represent a series of horizontal reflections within the ~4 ns interval of penetration. Their middle parts are registered approximately at the same time delays, which is particularly evident after applying the horizontal reflection filtering.

In addition to *1* and *2*, an intense reflection boundary *5* is distinctly observed in the upper part of the section, which is likely to be related to the position of the horizon which supplies freshwater via seepage during the intense melting of sea ice cover. This boundary represents a series of horizontal reflections characterized by about 4 ns penetration interval and their middle part position in the hole area at a

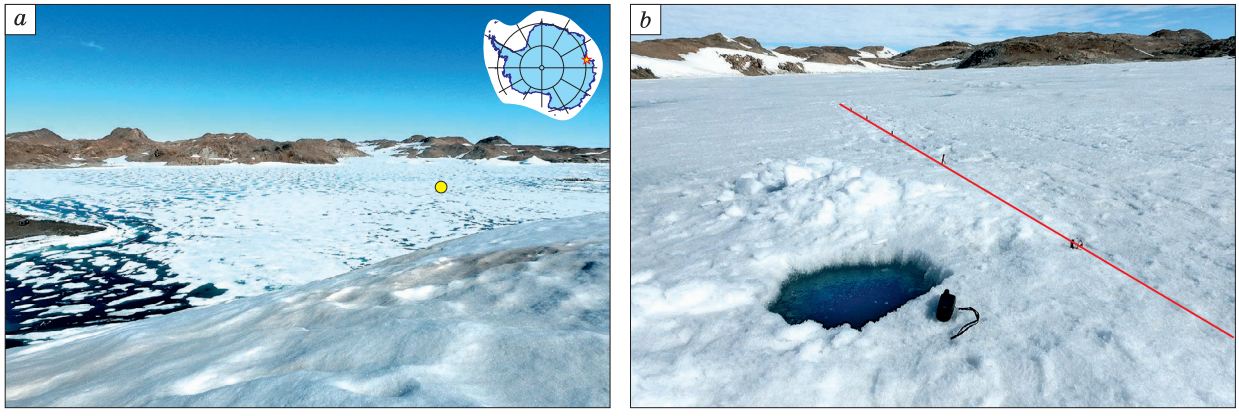

Fig. 1. Location of the acquisition test works on the Nella Fjord sea ice.

The area of works is shown in yellow circle; the red line marks the fragment of survey line in the vicinity of the maina. Photograph by S.V. Popov, Junuary 2017.

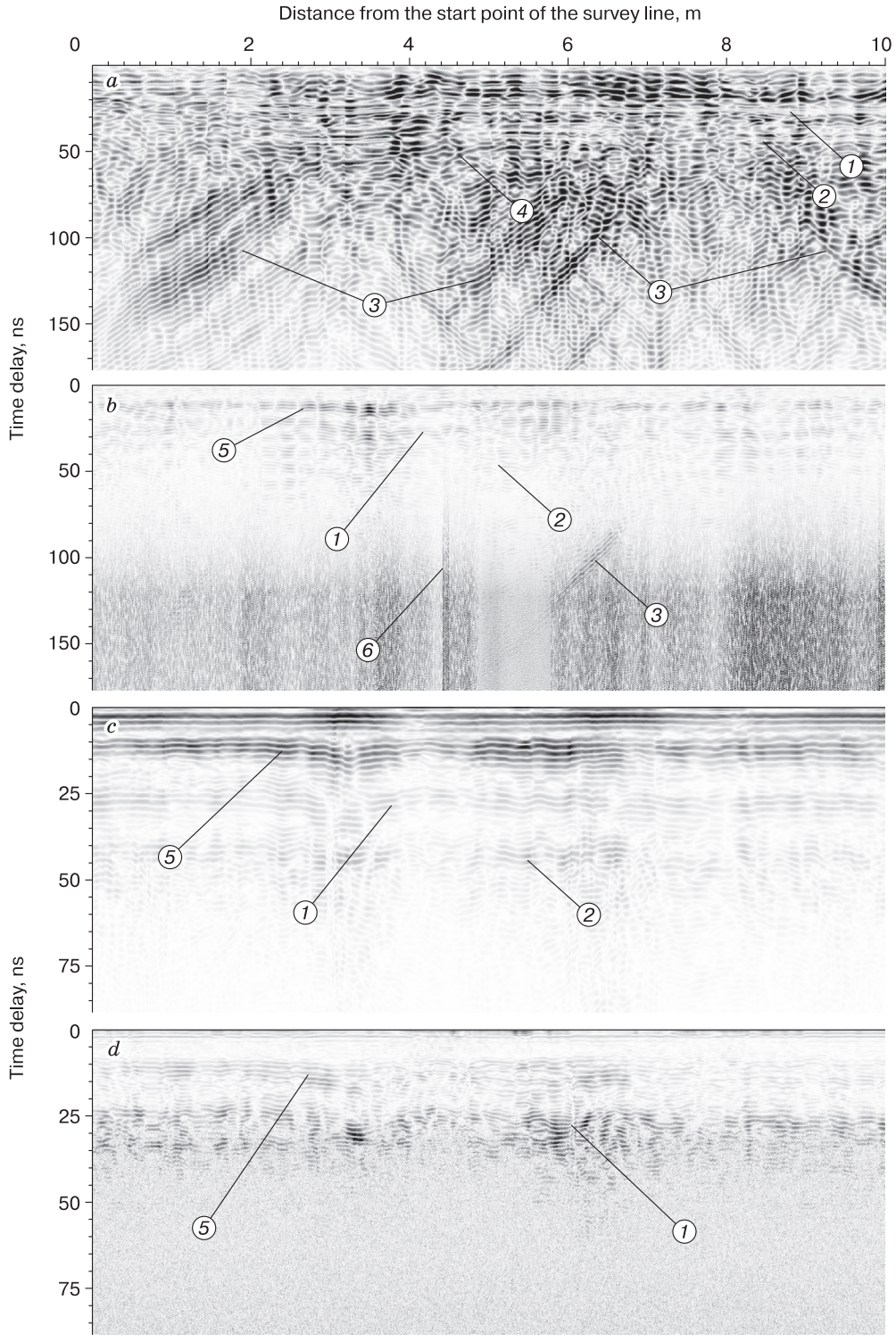

Fig. 2. GPR time sections resulting from the radar soundings using antenna frequencies of 150 MHz (*a*), 270 MHz (*b*), 400 MHz (*c*) и 900 MHz (*d*) during the acquisition works on the Nella Fjord sea ice.

1 – boundary between sea ice and seawater; *2* – boundary between fresh and seawater; *3* – diffractions from inhomogeneities; *4* – diffractions formed assumingly by the lower part of the maina; *5* – intra-ice boundary; *6* – noise from hand-held radio-station. The area of works is indicated in Fig. 1.

delay of about 12.3 ns. This is also distinctly visible in the previous time section (Fig. 2, *a*), but not explicitly differentiated in the mosaic structure of the wave field. Besides, the wavelength of the discussed radar sounding is almost twice as less than the previous one. This, in turn, means that the cross-section resolution in the first case is almost twice as worse than in the latter. This circumstance may be responsible for the apparent absence of contrast boundary *5* in the previous section (Fig. 2, *a*).

All but one diffracted waves *3*, reflected probably by the ice blocks, are absent from the time section. Vertical band *6* may have been caused the noise from a hand-held radio station.

Figure 2 shows a GPR time section obtained using 400 MHz frequency antenna, along with numerous sub-horizontal reflections, including *1* and *5*. A high quality visualization of boundary *2* required the nonlinear amplification of the reflection. To this end, the gain profile was set in such a way that only the second half of the section (from 50 ns delay and lower) was amplified to the value of 16 dB.

As is known, specific absorption of electromagnetic waves in dissipative media increases with frequency [*Finkelstein et al., 1977; Lebedev and Sukhorukov, 2001; Macheret, 2006*]; therefore, with its growth below boundary 1, the reflections are found to be fewer and fewer in number (Fig. 2). While fresh water, even very low mineraliazed, is characterized by a significant specific absorption of electromagnetic waves [*Bogorodskii et al., 1970a,b*].

In particular, for Lake Ladoga's water (Leningrad region), this parameter increases with higher antenna frequency: 21 dB/m (at the frequency of 400 MHz), 38 and 40 dB/m (900 MHz), 48 dB/m (1500 MHz) for different series of the experiments [*Popov et al., 2017*]. It can therefore be inferred that the medium in the span between boundaries *1* and *2*, is very likely interpreted to be melt water with low mineralization. As is the case with the above examples, boundaries *1, 2* and *5* occur in the same time window intervals, and no diffracted waves are registered on the time section. Figure 2, *d* represents a 900 MHz frequency GPR time-section, where likewise in other sections, a series of subhorizontal reflections *1* and *5* is imaged. Reflections below *1* are not observed due to a significant absorption of waves and their scattering on the inhomogeneities.

VELOSITY MODEL OF THE MEDIUM

GPR surveying is noted for an important, which is sometimes critical, issue of choice of a high-velocity model of the medium for correct time-to-depth conversion. Specifically, the information about velocity (dielectric permittivity) enables identification of the objects detected by GPR data with particular structural and compositional complex. Without taking the table values into account, these parameters can be determined in two ways: using travel-time of diffracted waves reflected by inhomogeneities [*Glazovskii and Macheret, 2014*] and by multi-offset sounding [*Sheremetyev, 1989; Popov et al., 2001; Popov et al., 2003; Vladov and Starovoitov, 2004; Macheret, 2006; Glazovskii and Macheret, 2014*]. The former is commonly used because of its simplicity and efficiency, whereas it is found not always applicable in practice. Using this method requires having at least a diffracted wave with extended branches, which could provide for calculations with sufficient accuracy. However, experience shows that these features of diffracted waves is the exception rather than the rule. In this case, the reflectors have to be evenly spread throughout the depth of the studied section, which is quite rare. Besides, obtaining a high-quality high-velocity model of the environment, ideally, involves a high-precision horizontal positioning of each sounding point, which is not always put into practice and largely depends on the tasks of the works.

Multi-offset sounding, carried out using the common depth point (CDP) or common source point (CSP) methods, is advantageous from the above approach, as it can be performed almost anywhere. The profile marking provides high accuracy. The velocity model of the medium based on these methods can therefore claim to be the most accurate. As an example, the results of the study of subglacial Lake Vostok (Eastern Antarctica), where this method was used to measure the glacier thickness in the area of drilling well 5G [*Popov et al., 2001, 2003*]. The relative error of the measurements revealed after the penetration of the lake was less than 0.5 % [*Popov et al., 2012*].

The CDP mode of radar sounding involves successive measurements while moving the transmitting/receiving antennas at the same distance from the array center. The application of the CSP method suggests that the position of one of the antennas is fixed, while the second is being moved along the survey line at its both sides [*Boganik and Gurvich, 2006*]. It is difficult to unambiguously assess which of them is better in terms of GPR applications. On the one hand, the second is easier to implement, allowing obtaining twice as bigger travel-time curve and is capable of more fully taking into account the dipping angle of the target boundaries.

On the other hand, when performing work on this technique, the reflection and refraction points of the waves move along the boundaries of the media in a much larger interval than in the first case. This, in turn, leads to the fact that the degree of deviation of their configuration from the straight line affects the quality of the result for the CSP to a greater extent than for the CDP system. Antennas AB-150 used with Russian OKO-2 GPR are extensible and their design features include fiber optic cable connecting

both antennas (transmitter/receiver). In our case, a 10 m cable was sufficient, which allowed sounding by any of the above methods, providing for the maximum array length. In the works performed on sea ice, the CDP method was applied with a minimum (80 cm) and maximum (980 cm) distance between the antennas, dictated by the design specifics of the antennas. Their offset along the profile was 10 cm. The calculations were performed within the framework of the dipping-layer model whose mathematical provision is given in [*Popov, 2017*].

Figure 3, *a* shows a GPR time-section obtained during the CDP soundings, while GPR profiling was performed at a frequency of 150 MHz. As is seen in Fig. 2, *a* the time section obtained using the same tools, abounds with noise waves, masking the target boundaries. These are so intense that for a more reliable resolution of the section, a horizontal filtering was applied.

These types of noise, though to a lesser extent, are also observed on the GPR time-section resulting from the CDP soundings (Fig. 3, *a*), which, however, were found quite difficult to suppress. The required traveltimes were picked as the most contrast reflections, at this the delays of the reflected signal at a minimum separation of antennas must coincide with the boundaries identified during the profiling (Fig. 2).

Theoretical hodograph (traveltime curve) *1* on the radargram shown in Fig. 3, *a* corresponds to a direct signal, i.e. an electromagnetic wave propagating through the air between the antennas. Given that it is emitted and registered by the side lobes, it appears very weak and becomes discernible on the GPR time-section only when strongly amplified.

Theoretical hodograph *2* in Fig. 3, *a* corresponds to the boundary occurring at a depth of 1.1 m, and to the *effective* dielectric permittivity of the overlying medium $\tilde{\varepsilon}=10$. In his publication, H. Looyenga [*1965*] calculated the ratio linking this parameter with a volumetric moisture content w for a two-component mixture "ice–water" with dielectric permittivities ε_i and ε_w, respectively:

$$\tilde{\varepsilon}=\left[\varepsilon_i^{1/3}+w\left(\varepsilon_w^{1/3}-\varepsilon_i^{1/3}\right)\right]^3.$$

The water inclusions are assumingly spherical. Graphically, this ratio is represented in Fig. 4. According to this model, the obtained value of permittivity corresponds to ice with a volumetric water content of 23.5 %. That high value is accounted for the

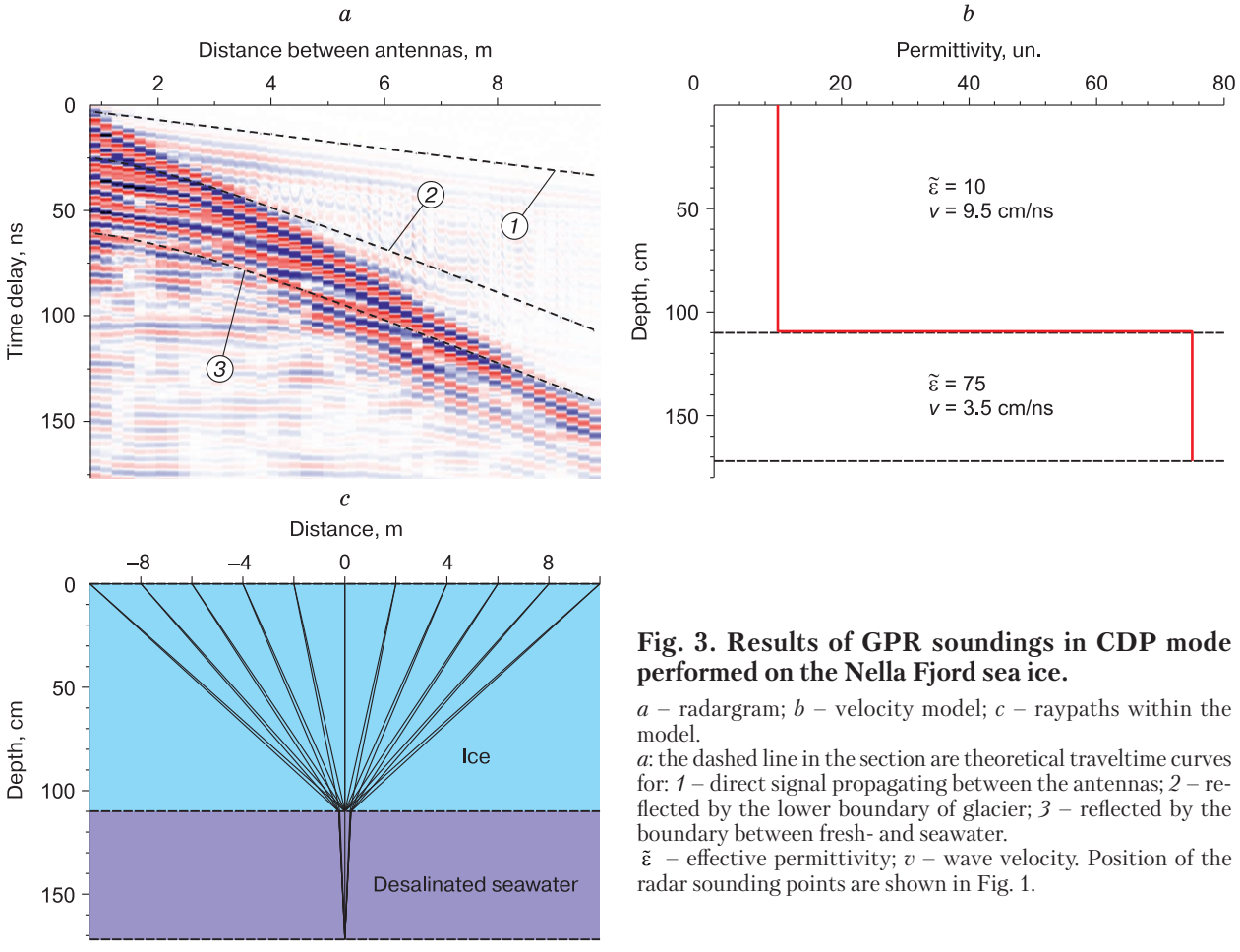

Fig. 3. Results of GPR soundings in CDP mode performed on the Nella Fjord sea ice.

a – radargram; *b* – velocity model; *c* – raypaths within the model.

a: the dashed line in the section are theoretical traveltime curves for: *1* – direct signal propagating between the antennas; *2* – reflected by the lower boundary of glacier; *3* – reflected by the boundary between fresh- and seawater.

$\tilde{\varepsilon}$ – effective permittivity; v – wave velocity. Position of the radar sounding points are shown in Fig. 1.

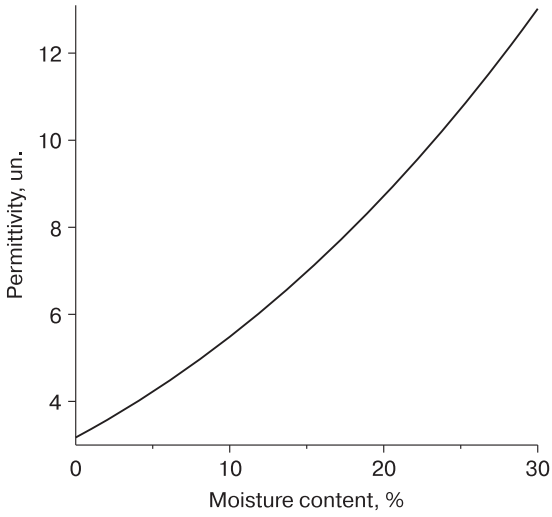

Fig. 4. A relationship between permittivity of the two-component ice-water mixture and volumetric content of moisture [*Looyenga, 1965*].

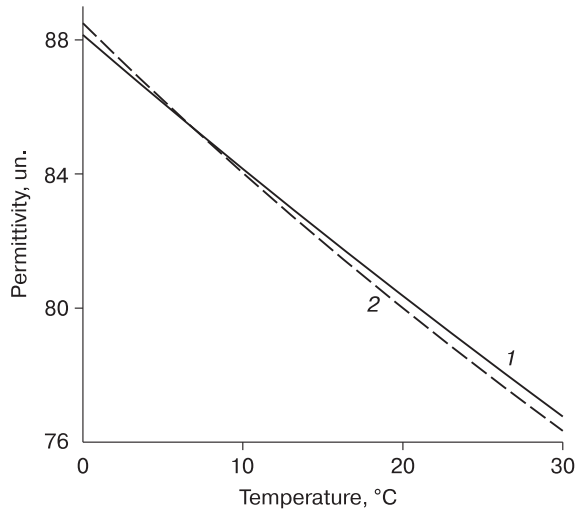

Fig. 5. A relationship between permittivity of freshwater and temperature for different empirical models:

1 – after [*Ray, 1972*]; *2* – after [*Chernyak, 1987*].

fact that, according to field observations, the near-surface part of the glacier contained a lot of melt water, which was seeping and then pouring into the ice-hole.

Theoretical hodograph *3* in Fig. 3, *a* corresponds to the boundary at a depth of 1.72 m, and the effective dielectric permittivity of the overlying medium ($\tilde{\varepsilon} = 75$). The obtained high value can only be associated with the melt water. On the other hand, the value is too low for it. The empirical correlation given in [*Ray, 1972*] is based on the relationship between dielectric constant of water ε_w and temperature T:

$$\varepsilon_w = 78.54\left(1 - 4.579\cdot10^{-3}\tilde{T} + 1.19\cdot10^{-5}\tilde{T}^2 - 2.8\cdot10^{-8}\tilde{T}^3\right),$$

where $\tilde{T} \equiv T - 25$.

The close values can be obtained from the empirical formula of G.Ya. Chernyak [*1987*]:

$$\varepsilon_w = 80 \Big/ \left[1 + 0.0048\left(T - 20\right)\right].$$

The $\varepsilon_w(T)$ ratios for each of these relationships in the meter-decimeter wavelength range are shown in Fig. 5, from which it follows that the dielectric constant of water is $\varepsilon_w \approx 88$ at the melting temperature.

The noted difference can be explained by the fact that the lower surface of sea ice is not smooth, which is evidenced, in particular, by the diffracted waves shown in Fig. 3, *a*, and the configuration of the target boundaries is shown in Fig. 2. The presence of ice blocks, characterized by a high velocity of electromagnetic waves, is sufficient for reducing the effective dielectric permittivity of the entire overlying layer.

However, we have another explanation for the target boundaries roughness (Fig. 2). Even if the physical boundaries are smooth (though it is unlikely), the effective permittivity can change along the section, and hence the effective velocity of electromagnetic waves propagation. These values are known to be very sensitive to the moisture content [*Macheret, 2006*]. The boundaries' unevenness may therefore be caused by the uneven distribution along the section of free water with depth, which can be associated also with the *lateral filtration* of melt water into the ice-hole, rather than with the glacier structure alone. In particular, the drilled well into the aquifer or oil reservoir provokes the liquid rushing into it [*Pyatibrat, 2012*], for which ample evidence was provided, in practice. This, in turn, means that after the placement of a well (or ice-hole, in our case), the distribution of melt water in the sea ice will be subjected to changing, causing thereby deformation of the target boundaries in the GPR time section. Similar changes were observed by the authors in open cracks [*Popov and Polyakov, 2016*].

There is, nevertheless, no doubt that this thin layer is desalinated seawater. The velocity model of the medium is imaged by Fig. 3, *b*, while raypaths propagation in the medium is shown in Fig. 3, *c*.

RESULTS OF OCEANOGRAPHIC STUDIES

The oceanographic survey route was outlined in one of the points for the AARI oceanographic surveys, where a day before the temperature measurements and seawater salinity were taken in maina by

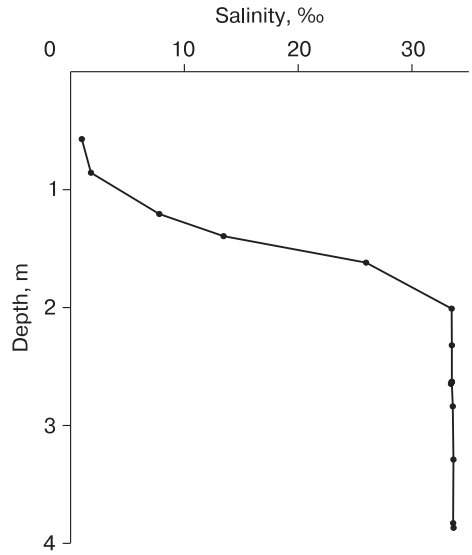

Fig. 6. Salinity profile for the near-surface part of Nella Fjord.

the Autonomous Profiler SeaCAT 19 plus V2 (SeaBird Scientific, USA). The profile of the latter is shown in Fig. 6.

It follows that in the range of depths from 1.6 to 2.0 m there is a fairly contrasting boundary between desalinated and sea water. According to the existing theoretical concepts of the processes of electromagnetic wave propagation, such boundary should be observed on the time GPR section, which was confirmed by the results of this work.

The fairly warm Antarctic summer of 2016/17 was has led to intensive melting of surface sea ice and therefore to its significant saturation by fresh water, as well as to desalination of the surface layer of seawater. This process was corroborated by both GPR and oceanographic data.

CONCLUSION

The integrated geophysical and oceanographic studies conducted during the 62nd (2016/17) RAE summer field season have confirmed good prospects of applicability of the electromagnetic sounding method by the industrial-scale ground-penetrating radars to the studies of the sea ice and determination of thickness of the desalinated layer of seawater. They showed that radar soundings of relatively thin (about 1 m) sea ice are performed at low frequencies (up to 400 MHz).

We find it feasible that for investigating thicker ice GPR profiling should be performed at one meter range frequencies. Besides , the studies have corroborated the possibility of determining the boundary position between fresh- and seawater by remote electromagnetic methods.

As mentioned above, GPR studies were conducted earlier in the area of the Molodezhnaya field base [*Popov and Polyakov, 2015*]. It should be noted that if the works discussed in this article were carried out in almost ideal conditions (all boundaries were subhorizontal and relatively smooth), the studies in the area of Molodezhnaya base were conducted on ice prone to ridging.

This tends to have essentially adverse effect on any remote studies. Nevertheless, even in this case, reflections from the surface of lower edge of ice, though not totally contrasting and confident, were obtained [*Popov and Polyakov, 2015*].

The above reasoning indicates good prospects for the GPR surveying method applicability to investigations of sea ice. However, bearing in mind that salt seawater creates a shield for electromagnetic waves propagation, the positive results in both cases were achieved only through intensive surface sea ice cover melting, which led to desalination of the upper part of the water column and made it passable to electromagnetic waves. As such, the quality results are unlikely to be obtained in winter, when desalination of seawater is arrested.

The authors would like to thank the management of the Russian Antarctic expedition and A.V. Mirakin, the head of Progress station, as well as their colleagues – G.G. Arshakyan, D.P. Blyakharsky, A.V. Drobyazko, A.I. Kutsurubu and N.V. Samdalyuk, the 62nd RAE participants for assistance in conducting this study. The authors also express their gratitude to the staff of the editorial group of the Earth's Cryosphere journal – to N.V. Arutyunyan and E.Y. Sokolova for the corrections effected to the paper, which undoubtedly improved it.

The work was supported by the Russian foundations for Basic Research (Project No. 17-55-12003 NNIO-a).

References

Bobrov, N.Yu., Dmitriev, V.V., Krylov, S.S., et al., 2008. New possibilities for GPR application to hydrogeological investigations of freshwater reservoirs. Vestnik SPbGU, Series 7, issue 2, pp. 76–81.

Boganik, G.N., Gurvich, I.I., 2006. Seismic Exploration. Izd-vo AIS, Tver, 744 pp. (in Russian)

Bogorodskii, V.V., Trepov, G.V., Fedorov, B.A., et al., 1970a. The use of EM wave propagation in fresh water for active detection and other purposes. Tr. AANII, 295, 116–119.

Bogorodskii, V.V., Trepov, G.V., Fedorov, B.A., et al., 1970b. Radar sounding measurements in fresh water. Tr. AANII, 295, 185–187.

Chernyak, G.Ya., 1987. Electromagnetic Methods in Hydrogeology and Engineering Geology. Nedra, Moscow, 211 pp. (in Russian)

Finkelshtein, M.I., Mendelson, V.L., Kutev, V.A., 1977. The Radar Observations of Layered Ground Covers. Sovetskoye radio, Moscow, 176 pp. (in Russian)

Galley, R.J., Trachtenberg, M., Langlois, A., et al., 2009. Observations of geophysical and dielectric properties and ground penetrating radar signatures for discrimination of snow, sea ice and freshwater ice thickness. Cold Reg. Sci. Technol. 57 (1), 29–38, DOI: 10.1016/j.coldregions.2009.01.003.

Glazovskii, A.F., Macheret, Y.Y., 2014. Water in Glaciers. Methods and results of geophysical and remote investigations. GEOS, Moscow, 527 pp. (in Russian)

GSSI, Antennas Manual, 2014. Geophysical Survey Systems, Inc., Salem, NH, MN30-903 Rev. E, 99 pp.

Haas, C., 2004. Late-summer sea ice thickness variability in the Arctic Transpolar Drift 1991–2001 derived from ground-based electromagnetic sounding. Geophys. Res. Lett., 31, L09402, DOI: 10.1029/2003GL019394.

Haas, C., Gerland, S., Eicken, H., et al., 1997. Comparison of sea-ice thickness measurements under summer and winter conditions in the Arctic using a small electromagnetic induction device. Geophysics, 62 (3), 749–757.

Haas, C., Lobach, J., Hendricks, S., et al., 2009. Helicopter-borne measurements of sea ice thickness, using a small and lightweight, digital EM system. J. Appl. Geophys. 67 (3), 234–241.

Holt, B., Kanagaratnam, P., Gogineni, S.P., et al., 2009. Sea ice thickness measurements by ultrawideband penetrating radar: First results. Cold Reg. Sci. Technol. 55 (1), 33–46.

Lebedev, G.A., Sukhorukov, K.K., 2001. EM and Acoustic Waves Propagation in Sea Ice. Gidrometeoizdat, Saint Petersburg, 82 pp. (in Russian)

Lee, Y.J., Lim, W.K., Ewe, H.T., 2011. A study of an inversion model for sea ice thickness retrieval in Ross Island, Antarctica. Prog. Electromagn. Res. 111, 381–406.

Looyenga, H., 1965. Dielectric constants of heterogeneous mixture. Physica 31 (3), 401–406.

Macheret, Y.Y., 2006. Radio echo sounding of Glaciers. Nauchny Mir, Moscow, 392 pp. (in Russian)

Panzer, B., Gomez-Garcia, D., Leuschen, C., et al., 2013. An ultra-wideband, microwave radar for measuring snow thickness on sea ice and mapping near-surface internal layers in polar firn. J. Glaciol. 59 (214), 244–254.

Panzer, B., Leuschen, C., Patel, A., et al., 2010. Ultra-wideband radar measurements of snow thickness over sea ice, in: Proc. of 2010 IEEE Intern. Geoscience and Remote Sensing Symp., pp. 3130–3133, DOI: 10.1109/IGARSS.2010.5654342.

Popov, S.V., 2017. Determination of dielectric permittivity from diffraction traveltime curves within a dipping-layer model. Earth's Cryosphere XXI (3), 75–79.

Popov, S.V., Kashkevich, M.P., 2015. Two-position sounding in ground-penetrating radar technique: restrictions and possibilities. Probl. Arktiki i Antarktiki 105 (3), 99–110.

Popov, S.V., Kashkevich, M.P., Kashkevich, V.I., et al., 2017. Absorption of UHF electromagnetic waves in the water of Lake Ladoga (Leningrad region). Problemy Arktiki i Antarktiki 112 (2), 43–49.

Popov, S.V., Masolov, V.N., Lukin, V.V., et al., 2012. Russian seismic, radio and seismological investigations of subglacial Vostok Lake. Led i Sneg 4 (120), 31–38.

Popov, S.V., Mironov, A.V., Sheremet'yev, A.N., et al., 2001. Measurements of mean velocity of EM wave propagation in glacier ice at Vostok station. Mater. Glyatsiol. Issled. Issue 90, 206–208.

Popov, S.V., Polyakov, S.P., 2015. Results of glaciological GPR research and methodology works in the area of the Antarctic field base Molodezhnaya station in the season of the 60th RAE (2014/15). Problemy Arktiki i Antarktiki 106 (4), 54–62.

Popov, S.V., Polyakov, S.P., 2016. GPR sounding of ice crevasses of the area of the Russian Progress and Mirny stations (East Antarctica) during the field season of 2014/2015. Earth's Cryosphere XX (1), 82–90.

Popov, S.V., Sheremet'ev, A.N., Masolov, V.N., et al., 2003. Velocity of radio-wave propagation in ice at Vostok station, Antarctica. J. Glaciol. 49 (165), 179–183.

Pyatibrat, V.P., 2012. Foundations of Subsurface Hydromechanics. UGTU, Ukhta, 123 pp. (in Russian)

Radiotechnical device OKO-2 for subsurface scanning (Ground Penetrating Radar, GPR), 2009. Technical specification. OOO Logicheskie Sistemy (Logical Systems), Ramenskoye, 94 pp. (in Russian)

Ray, P.S., 1972. Broadband complex refractive indices of ice and water. Appl. Opt. 11 (8), 1836–1844, DOI:10.1364/AO.11.001836.

Sheremeyev, A.N., 1989. Measuring velocity of electromagnetic waves propagation in glacier on Dome B in Antarctica. In: Bogorodskii, V.V., Gavrilov, V.P. (Eds.). Elektrofizicheskie i fiziko-mekhanicheskie svoistva lda (Electro-physical and physico-mechanical properties of ice). Gidrometeoizdat, Leningrad, pp. 59–64. (in Russian)

Vladov, M.L., Starovoitov, A.V., 2004. Introduction to GPR survey. Moscow University Press, Moscow, 153 pp. (in Russian)

Received March 23, 2017